

## Chapter 2

# Modeling Collagen-Proteoglycan Structural Interactions in the Human Cornea

Xi Cheng, Hamed Hatami-Marbini, and Peter M. Pinsky

**Abstract** The cornea is a supremely organized connective tissue making it ideal for modeling and probing possible roles of collagen-PG interactions in the extracellular matrix. The cornea can be viewed as a reinforced electrolyte gel involving molecular-scale interactions between collagen fibrils, proteoglycans (PGs) and the mobile ions in the interfibrillar space. The swelling property of the tissue cannot be adequately predicted by Donnan theory for osmotic pressure. We propose an alternative unit cell approach based on a thermodynamic framework that employs a mean-field approximation for the electrostatic free energy and which accounts for a non-uniform electrostatic potential. The model is used to show that the equilibrium swelling pressure can be explained when the geometrical effect of electrolyte exclusion due to collagen fibril volume is considered. The model is further refined by dividing the PGs into collagen fibril coating and volumetric partitions. The model suggests that the PG coatings overlap at low hydration and set up repulsive forces that may act to maintain the collagen lattice order. Finally, we introduce a molecular-level unit cell in which volumetric domains within the unit cell are associated with the macromolecular GAGs and results from the continuum and molecular-level models are compared.

---

X. Cheng · H. Hatami-Marbini · P.M. Pinsky (✉)

Department of Mechanical Engineering, Stanford University, 496 Lomita Mall,  
Stanford, CA, USA

e-mail: [pinsky@stanford.edu](mailto:pinsky@stanford.edu)

X. Cheng

e-mail: [cx1012@stanford.edu](mailto:cx1012@stanford.edu)

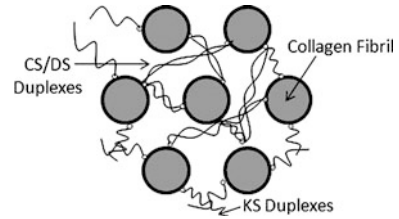
*Present address:*

H. Hatami-Marbini

School of Mechanical and Aerospace Engineering, Oklahoma State University,  
218 Engineering North, Stillwater, OK, USA

e-mail: [hhatami@okstate.edu](mailto:hhatami@okstate.edu)

**Fig. 2.1** Collagen-PG arrangement in the corneal stroma; some of the GAG chains may bridge fibrils by antiparallel duplexing (Scott, 1992)



## 2.1 Introduction

The extracellular matrix of the cornea is composed of two principal molecular components: type I collagen in the form of 25 nm diameter fibrils and small leucine-rich repeat proteoglycans (PGs). The corneal stroma is organized into approximately 500 lamellae (or fibers) through its thickness and within each lamella the collagen fibrils are maintained in almost perfect parallel arrays with a quasi-regular hexagonal packing arrangement. The collagen is responsible for carrying the tensile forces that are produced by the intraocular pressure. The corneal PGs consist of linear chains of disaccharide units covalently bound to a core protein. Predominant corneal glycosaminoglycan (GAG) components are dermatan sulfate (DS), chondroitin sulfate (CS) and keratan sulfate (KS). Scott (1992) proposed that some GAGs form interfibrillar bridges by duplexing and this has been supported by some evidence from imaging (Muller et al., 2004; Lewis et al., 2010). These arrangements are illustrated in Fig. 2.1. The DS, CS and KS disaccharide units are ionized at physiological pH and carry two negative charges per unit. The electrostatic interaction of these charges with ionic species gives rise to strong intermolecular forces that are responsible for the tissue osmotic pressure.

The transparency of the cornea requires that the collagen fibrils be maintained in their lattice-like arrangement. Modeling the forces of interaction between the collagen fibrils and GAGs may provide insights into the mechanisms underlying corneal transparency and is a primary goal of this work. The polyelectrolyte nature of the corneal stroma is well illustrated by its remarkable capacity for swelling when immersed in water or dilute salt solution. The tendency of the corneal stroma to swell can be characterized by the equilibrium swelling pressure. The equilibrium swelling pressure may be measured by compressing a piece of isolated corneal stroma in an ionic bath solution between permeable plates until equilibrium is reached (Hedbys and Dohlman, 1963). During the past several decades, the swelling pressure on various species have been measured experimentally (Hedbys and Dohlman, 1963; Fatt, 1968; Olsen and Sperling, 1987), and it has been observed that the swelling pressure is highly dependent on the tissue hydration.

Several previous investigations have aimed to create theoretical models for corneal swelling (Hart and Farrell, 1971; Hodson, 1971; Olsen and Sperling, 1987). It has been demonstrated that Donnan theory for osmotic pressure is incapable of fully explaining swelling pressure (Olsen and Sperling, 1987). In this work we propose a swelling pressure theory that is derived from a molecular-level description of

the polyelectrolyte system that recognizes the spatial heterogeneity of charge density that exists in the tissue. A similar thermodynamic approach was employed by Hart and Farrell (1971), but the present work uses an entirely different description of the electrostatic free energy. The electrostatic free energy of a polyelectrolyte found through a mean-field approximation can be expressed as a functional of the electrostatic potential, fixed charge density and local ionic concentrations (Che et al., 2008). The electrostatic potential is determined from solution of the Poisson-Boltzmann equation over a unit cell and the swelling pressure is found as the gradient of the free energy with respect to the swelling volume. By considering the volumetric domains of polyelectrolyte excluded by the collagen fibrils, the model finds excellent agreement with the experimental swelling pressure data.

In order to improve the model for low levels of hydration, we were lead by experimental observations to postulate that the stromal PGs are partitioned into two sets. One set is associated with PGs that bridge (perhaps by duplexing of the longer DS and CS GAGs) between neighboring collagen fibrils; these supply the charge density responsible for the osmotic pressure at physiological hydration. A second set produces a charge-rich coating around the collagen fibrils (perhaps formed primarily by the shorter KS GAGs). At physiological hydration, the coatings do not interact and add very little to the osmotic pressure. As hydration is reduced, the collagen fibrils come into closer proximity and the coatings will overlap producing a significant increase in local charge density and a concomitant increase in swelling pressure and electrostatic repulsion. We conclude that the PG-coatings may represent a mechanism to order the collagen fibril lattice as required in order for the cornea to be a good transmitter of light.

## 2.2 Comparison of Donnan and Poisson-Boltzmann Theories Applied to the Cornea

### 2.2.1 Donnan Theory

If a polyelectrolyte phase is in equilibrium with an external bath ionic solution, osmotic pressure will result from the polyelectrolyte fixed charges and the disparity of ionic concentrations in the two phases. Donnan theory may be employed to model the osmotic pressure under the assumption that the fixed charge density is spatially invariant. Consider a sample of isolated corneal stroma placed in a NaCl bath. Assuming ideal Donnan equilibrium, the distribution of mobile ions satisfies

$$\bar{C}_{\text{Na}^+} \bar{C}_{\text{Cl}^-} = C_0^2, \quad (2.1)$$

where  $\bar{C}_{\text{Na}^+}$  and  $\bar{C}_{\text{Cl}^-}$  are the mobile ion concentrations in the stroma and  $C_0$  the ionic concentration in the bath. The GAG disaccharide units provide a fixed (non-mobile) negative charge density  $\rho_f$  and electroneutrality within the polyelectrolyte

phase requires,

$$\bar{C}_{\text{Na}^+} - \bar{C}_{\text{Cl}^-} + \frac{\rho_f}{F} = 0, \quad (2.2)$$

where  $F$  is the Faraday constant. Equations (2.1) and (2.2) can be solved for the equilibrium mobile ion concentration (Buschmann and Grodzinsky, 1995) giving

$$\bar{C}_{\text{Na}^+/\text{Cl}^-} = \mp \frac{\rho_f}{2F} + \sqrt{\frac{\rho_f^2}{4F^2} + C_0^2}. \quad (2.3)$$

The osmotic pressure in the two phases is given by

$$P_{\text{poly}} = RT(\bar{C}_{\text{Na}^+} - \bar{C}_{\text{Cl}^-}), \quad P_{\text{bath}} = 2RT C_0, \quad (2.4)$$

where  $R$  is the gas constant and  $T$  is the absolute temperature. The osmotic pressure difference  $P_{\text{os}}$  between the two phases is then computed as

$$P_{\text{os}} = P_{\text{poly}} - P_{\text{bath}} = 2RT C_0 \left( \sqrt{\frac{\rho_f^2}{4F^2 C_0^2} + 1} - 1 \right). \quad (2.5)$$

In Fig. 2.2 we depict experimental measurements and fitting curves for the equilibrium swelling pressure of human corneal stroma with a bath concentration of  $C_0 = 0.15$  M as reported by Hedbys and Dohlman (1963) and Olsen and Sperling (1987). Letting  $\rho_0$  represent the fixed charge density at physiological sample thickness  $t_0 = 0.5$  mm, and letting  $\rho_f$  represent the charge density at tissue sample thickness  $t$ , we find by conservation of fixed charge that  $\rho_f = \rho_0(t_0/t)$ . Using this result in Eq. (2.5), the osmotic pressure difference at thickness  $t$  may be estimated in terms of the physiological fixed charge density  $\rho_0$ . It has been shown that  $\rho_0$  depends on the salt concentration in the bath through a process of ion binding. Hodson (1971) has estimated  $\rho_0/F$  for human stroma at physiological hydration and bath ionic concentration  $C_0 = 0.15$  M to be approximately 48 mM. Values of  $\rho_0/F$  for bovine cornea have been measured at around 36 mM; see Elliott and Hodson (1998) for a review. The osmotic pressure difference  $P_{\text{os}}$  based on Donnan theory Eq. (2.5) with  $\rho_0/F = 48$  mM is shown in Fig. 2.2. The prediction agrees well with the experimental data at physiological thickness  $t = 0.5$  mm but deviates significantly for all other values, particularly for  $t < 0.5$  mm. We conclude that Donnan theory is incapable of predicting swelling pressure accurately for lower thicknesses, which correspond to hydration levels lower than physiological.

### 2.2.2 Poisson-Boltzmann Theory

We now consider a thermodynamic framework for describing the swelling pressure experiment on corneal stroma. Consider a sample of isolated corneal stroma of area

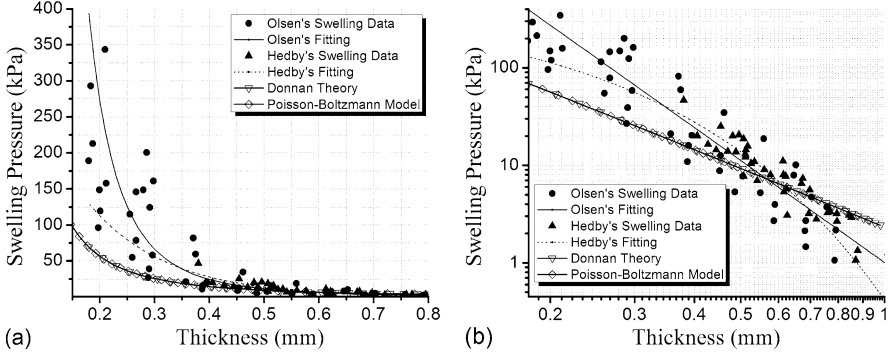


**Fig. 2.2** Swelling pressure vs. thickness by Hedbys and Dohlman (1963) and Olsen and Sperling (1987), the Donnan model and the Poisson-Boltzmann (PB) model. Data plotted on the normal axis (a) and a log-log axis (b). Fitting curve by Olsen:  $P_s = 7.56 \times t^{-3.48}$  mmHg and the fitting curve based on Hedbys' data (Fatt, 1968)  $P_s = 1810 \times \exp(-H)$  mmHg. The hydration data from Hedbys and Dohlman (1963) is transformed to thickness by the linear relation  $H = 7.00t - 0.64$  (Hedbys and Mishima, 1966). Charge density for Donnan model and the PB model is  $\rho_0/F = 48$  mM

$A_s$  immersed in an ionic solution and constrained by a porous piston to a thickness  $t$ . The total Gibbs free energy of the system is defined as

$$\mathcal{G} = \mathcal{F} + PV + P_s A_s t, \quad (2.6)$$

where  $\mathcal{F}$  is the Helmholtz free energy,  $P$  and  $V$  are the atmosphere pressure and total system volume, respectively, and  $P_s$  is the pressure exerted by the piston on the sample (Katchalsky and Michaeli, 1955; Hart and Farrell, 1971). At equilibrium we require

$$P_s = -\frac{1}{A_s} \frac{\partial}{\partial t} (\mathcal{F} + PV). \quad (2.7)$$

At fixed temperature  $T$  and atmosphere pressure  $P$ , the  $PV$  term may be dropped and the swelling pressure is then expressed as

$$P_s = -\frac{1}{A_s} \frac{\partial \mathcal{F}}{\partial t} \bigg|_{T,P} = -\frac{\partial \mathcal{F}}{\partial V_t} \bigg|_{T,P}, \quad (2.8)$$

which is simply the derivative of the Helmholtz free energy with respect to the tissue volume  $V_t$ .

In general, the Helmholtz free energy  $\mathcal{F}$  will have electrostatic  $\mathcal{F}_{el}$  and chemo-mechanical components  $\mathcal{F}_{cm}$  (Jin and Grodzinsky, 2001). The effective electrostatic free energy of a polyelectrolyte solution in a mean-field approximation can be expressed as a functional of the electrostatic potential  $\varphi$  and local ionic concentrations

$C_1, \dots, C_M$  (Che et al., 2008)

$$\begin{aligned} \mathcal{F}_{\text{el}}[\varphi, C_1, \dots, C_M] = \int_{\Omega} \left\{ -\frac{\varepsilon}{2} |\nabla \varphi|^2 + \rho(r) \varphi + RT \sum_{i=1}^M C_i^{\infty} \right. \\ \left. + RT \sum_{i=1}^M C_i [\ln(\Lambda^3 N_A C_i) - 1] - \sum_{i=1}^M \mu_i N_A C_i \right\} d\Omega, \end{aligned} \quad (2.9)$$

where  $\varepsilon$  is the dielectric permittivity of the solution,  $N_A$  is the Avogadro constant,  $C_i^{\infty}$  and  $\mu_i$  are the bath concentration and chemical potential of the  $i$ th ionic species, respectively, and  $\Lambda$  is the thermal de Broglie wavelength. The local charge density  $\rho(r)$  is given by

$$\rho(r) = \rho_f(r) + \sum_{i=1}^M F z_i C_i(r), \quad (2.10)$$

where  $\rho_f$  is the fixed charge density from the GAG disaccharide units and  $z_i$  is the valence number for the  $i$ th ionic species. In Eq. (2.9), the first two terms are the internal electrostatic energy, the third term is the osmotic pressure from the mobile ions, the fourth term constitutes the ideal gas entropy and the last term accounts for the chemical potential. Setting the first variation of the free energy  $\mathcal{G}$  with respect to the concentration  $C_i$  to zero leads to

$$C_i(r) = C_i^{\infty} \exp\left(-z_i \frac{F\varphi(r)}{RT}\right), \quad (2.11)$$

which is the Boltzmann distribution for the concentrations at equilibrium. The variation of  $\mathcal{F}_{\text{el}}$  with respect to the potential  $\varphi$  yields the Poisson equation

$$\nabla \cdot \varepsilon \nabla \varphi(r) = -\rho(r). \quad (2.12)$$

The Poisson-Boltzmann equation (PBE) is obtained by combining Eqs. (2.10)–(2.12),

$$-\varepsilon \nabla^2 \varphi(r) = \rho_f(r) + \sum_{i=1}^M F z_i C_i^{\infty} \exp\left(-z_i \frac{F\varphi(r)}{RT}\right). \quad (2.13)$$

Substituting Eqs. (2.10), (2.11) into (2.9), the free energy at equilibrium is obtained as

$$\mathcal{F}_{\text{el}}[\varphi] = \int_{\Omega} \left\{ -\frac{\varepsilon}{2} |\nabla \varphi|^2 + \rho_f \varphi - RT \sum_{j=1}^M C_j^{\infty} \left[ \exp\left(-z_j \frac{F\varphi(r)}{RT}\right) - 1 \right] \right\} d\Omega. \quad (2.14)$$

It is remarked that this expression defines a concave functional; it has a unique equilibrium potential  $\varphi$  at which the functional is maximized (Fogolari and Briggs, 1997).

Specializing (2.13) and (2.14) to a binary electrolyte we find:

$$-\nabla^2 \varphi = \frac{\rho_f}{\varepsilon} - \frac{2FC_0}{\varepsilon} \sinh\left(\frac{F\varphi(r)}{RT}\right), \quad (2.15)$$

and

$$\mathcal{F}_{el} = \int_{\Omega} \left\{ -\frac{\varepsilon}{2} |\nabla \varphi|^2 + \rho_f \varphi - 2RTC_0 \left[ \cosh\left(\frac{F\varphi}{RT}\right) - 1 \right] \right\} d\Omega. \quad (2.16)$$

Returning to the equilibrium swelling pressure problem and taking (as in the Donnan solution) a uniform fixed charge density of  $\rho_f/F = 48$  mM and bath ionic concentration of  $C_0 = 0.15$  M, the swelling pressure was computed using Eq. (2.8) and the results are shown for varying sample thickness  $t$  in Fig. 2.2. The derivative of the free energy  $\mathcal{F}_{el}$  with respect to  $t$  was computed using central difference. As expected for this case of uniform charge density, the results are consistent with the Donnan prediction and confirm the thermodynamic framework provided by Eqs. (2.8) and (2.16).

### 2.2.3 An Unit Cell Model Based on Collagen Fibril Volume Exclusion

Both the Donnan and Poisson-Boltzmann (PB) theories confirm that the assumption of a spatially uniform charge distribution results in an unsatisfactory prediction of stromal swelling, especially for low levels of hydration. However, it is observed that the collagen fibrils occupy approximately 30 % of the stroma by volume (Meek and Leonard, 1993). As the tissue is compressed during the swelling pressure experiment, we argue that (i) the volume occupied of the collagen fibrils is unaffected by the change in stromal thickness, and (ii) the collagen fibrils maintain very few net ionized groups and contribute little or nothing to the electric balance within the tissue (Elliott and Hodson, 1998). Therefore, the GAG charges, which are conserved, must be restricted to the volumetric region between the collagen fibrils. Clearly, as the tissue is compressed, there will be a nonlinear increase in charge density due to the *geometric* effect of the collagen fibril volume exclusion.

Experimental estimation of the interfibrillar spacing  $l_c$  and radius of collagen fibril  $r_f$  in the human cornea suggest they lie in the ranges of  $45 \sim 60$  nm and  $11.5 \sim 15.0$  nm, respectively (Fratzl and Daxer, 1993; Elliott and Hodson, 1998; Muller et al., 2004). Consider a perfect hexagonal collagen lattice with  $l_c = 53.0$  nm and  $r_f = 12.5$  nm as shown in Fig. 2.3(a). Charge is now assumed to be uniformly distributed in the interfibrillar region  $\Omega_s \in \mathbb{R}^3$  only and is zero in the fibril domains. The PB equation (2.13) was solved on a sequence of unit domains  $\{\Omega_f^i\}$  in which

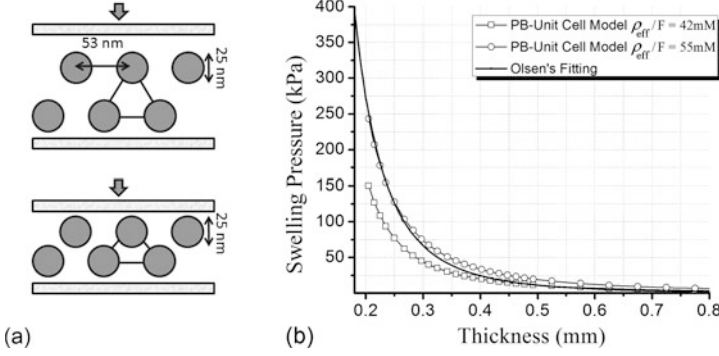


**Fig. 2.3** (a) 2D illustration of the unit cell, charge distribution is uniform over the interstitial region  $\Omega_s$ . The tissue is deformed by pressing the porous piston and the deformed unit cell is calculated from affine mapping; (b) Swelling pressure computed by PB-unit cell model based on collagen volume exclusion. The charge density is calibrated to be  $\rho_{\text{eff}}/F = 42 \sim 55$  mM. The lower and upper bound of the  $\rho_{\text{eff}}$  are determined by fitting the result at physiological situation ( $t = 0.5$  mm) and the low hydration situation ( $t = 0.2$  mm) respectively. The interfibril spacing  $l_c = 53$  nm and the collagen radius  $r_f = 12.5$  nm

the total fixed charge  $Q_f$  is conserved and the charge density computed from  $\rho_f^i = Q_f/V_f^i$ , where  $V_f^i$  is the volume of  $\Omega_f^i$ . The results are shown in Fig. 2.3(b) and labeled in terms of effective charge density  $\rho_{\text{eff}}$  defined by

$$\rho_{\text{eff}} = \frac{\rho_f V_f}{V_0}, \quad (2.17)$$

where  $V_0$  is the total volume of the unit cell including the fibril volume at physiological thickness. Values of  $\rho_{\text{eff}}/F = 42$  mM and 55 mM give best fits at physiological and low hydration, respectively, and produce predictions that are dramatically better than those of Donnan theory.

### 2.3 The Case for a PG-Coating of the Collagen Fibrils

Fratzl and Daxer (1993) describe X-ray scattering studies to measure the structural transformation of collagen fibrils under varying hydration produced by drying the tissue. The data strongly suggests that stromal PGs are heterogeneously distributed in the interfibrillar space. They appear in relatively high density in the vicinity of the fibrils where they may form a charge-rich effective PG coating surrounding each fibril. Hodson (1971) and Twersky (1975) have, much earlier, speculated on the existence of a such a fibril coating. Fratzl and Daxer (1993) estimated the radius of the coating as  $r_c = 18$  nm. Interestingly, they showed that the coating radius  $r_c$  is insensitive to hydration over a wide range and this suggests that the charge density associated with the coating PGs will not change with variations in hydration. However, at low levels of hydration the coatings may overlap and interact, as described below.



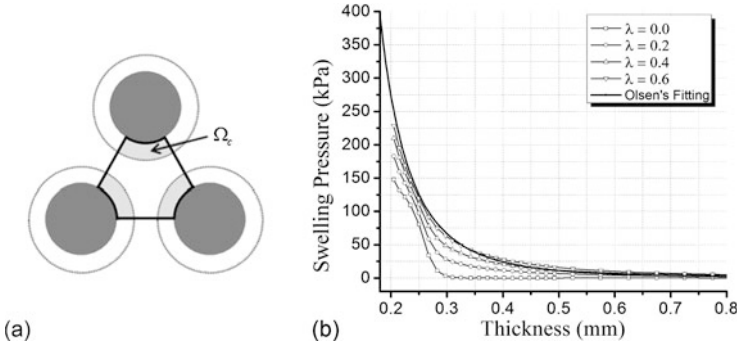


**Fig. 2.4** (a) 2D illustration of the coating unit cell. Charges are distributed into the coating region  $\Omega_c$  and the non-coating region  $\Omega^i \setminus \Omega_c$ . (b) Swelling pressure computed by the coating model under overall charge density  $\rho_{\text{eff}}/F = 55 \text{ mM}$ . The coating radius is set to be 18 nm, and the charge fraction  $\lambda$  for the bridging GAGs varies from 0.0 to 0.6. The optimal fitting occurs at  $\lambda = 0.6$

We propose a coating model in which the total unit cell charge  $Q$  is partitioned into two GAG-based classes: one based on charge derived from long interfibrillar bridging GAGs and one based on charge derived from short GAGs that form the coating. As in the previous model, we exclude the volume of the collagen fibrils in our analysis. A sequence of unit cell domains is defined by symmetry of the lattice and is denoted  $\Omega^i$  with volume  $V^i$ . Here  $i$  is a configuration index corresponding to tissue thickness (and thus hydration). The coating subregion of the unit cell is denoted  $\Omega_c$  and has volume  $V_c$ , which is *independent* of  $V^i$  in accordance with the findings of Fratzl and Daxer (1993). The setup is shown in Fig. 2.4(a). Letting  $\lambda \in [0, 1]$  denote the charge fraction parameter, the unit cell has two charge densities computed as follows

$$\rho_s^i = \lambda \frac{Q}{V^i} \quad (2.18)$$

over  $\Omega^i$ , and

$$\rho_c = (1 - \lambda) \frac{Q}{V_c} \quad (2.19)$$

over  $\Omega_c$ . Clearly, the total charge in the unit cell  $\Omega^i$  is conserved. Further, the coating charge density  $\rho_c$  is invariant with respect to hydration (i.e. index  $i$ ). If the coating subdomains overlap at low thickness values, we assume that the charge density is additive in the overlap region in order to conserve total charge. The boundary value problem to be solved on each unit cell domain  $\Omega^i$  is then

$$-\nabla^2 \varphi = \frac{\rho}{\varepsilon} - \frac{2FC_0}{\varepsilon} \sinh\left(\frac{F\varphi}{RT}\right), \quad \text{in } \Omega^i, \quad (2.20)$$

with the boundary conditions:

$$[|\varphi|] = 0, \quad [|\nabla\varphi \cdot \mathbf{n}|] = 0, \quad \text{on } \Gamma_{\text{inner}}, \quad (2.21)$$

$$\nabla\varphi \cdot \mathbf{n} = 0, \quad \text{on } \Gamma_{\text{outer}}, \quad (2.22)$$

and where  $\Gamma_{\text{inner}}$  and  $\Gamma_{\text{outer}}$  denote the inner and outer boundaries of the unit cell, respectively. The electrostatic free energy takes the form

$$\mathcal{F}_{\text{el}} = \int_{\Omega^i} \left[ -\frac{\varepsilon}{2} |\nabla\varphi|^2 + \rho\varphi - 2RT C_0 \left( \cosh\left(\frac{F\varphi}{RT}\right) - 1 \right) \right] d\Omega^i, \quad (2.23)$$

where the charge density distribution  $\rho$  in Eqs. (2.20) and (2.23) is given by

$$\rho^{(i)} = \begin{cases} \rho_s^i, & \text{in } \Omega^i \setminus \Omega_c, \\ \rho_s^i + \rho_c, & \text{on } \Omega_c, \\ 2(\rho_s^i + \rho_c), & \text{on } \Omega_{c-c}. \end{cases} \quad (2.24)$$

Here  $\Omega_{c-c}$  refers to the subdomain of  $\Omega_c$  resulting from the possible geometric intersection of coating domains as  $\Omega^i$  is mapped to correspond to lower thickness values with increasing index  $i$ .

In this model, the coating radius is taken to be  $r_c = 18.0$  nm. The effective charge density is again defined by  $\rho_{\text{eff}} = Q/V_0$  and used for reporting results. The influence of the charge fraction  $\lambda$  on the swelling pressure is shown in Fig. 2.4 at the physiologically plausible  $\rho_{\text{eff}}/F = 55$  nm. At  $\lambda = 0$ , all charge is concentrated in the coatings and the swelling pressure is zero until the coatings begin to interact at around  $t = 0.3$  mm. As  $\lambda$  is increased the swelling pressure increases monotonically toward the experimental curve. At a value of  $\lambda = 0.6$ , the computed swelling pressure finds excellent agreement with the experimental curve and further improves on the result of the previous section.

## 2.4 Molecular-Level Unit Cell Model

Here we present a molecular-level unit cell model which explicitly considers the GAG chains that are bridging neighboring collagen fibrils. In this model, the bridging GAGs domains are approximated by an effective cylindrical volume (Hart and Farrell, 1971; Jin and Grodzinsky, 2001). The non-bridging GAGs that constitute the collagen fibril coating are modeled, as above, with a continuum description of the charge density. The charge density within the cylindrical GAG domain is denoted  $\rho_g$  and is determined by three parameters: the half length of the GAG disaccharide unit  $b = 0.64$  nm (Jin and Grodzinsky, 2001), the cylinder radius  $r_g$  and a molecular ratio factor  $\alpha = L_c/L_d$ , where  $L_c$  is the contour length of the GAG chains and  $L_d$  is end-to-end distance. Then  $\rho_g$  may be computed from

$$\rho_g = \frac{\alpha e}{\pi b r_g^2}, \quad (2.25)$$

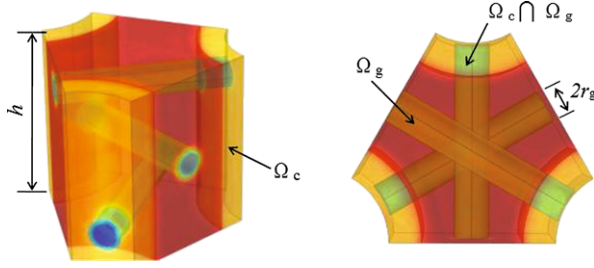


**Fig. 2.5** Illustration of the molecular-level unit cell. The collagen fibrils are connected by the GAGs via next-nearest neighbor connectivity. The subdomains are:  $\Omega_c \cap \Omega_g$ —the overlapping domain of the coating and interconnecting GAGs;  $\Omega_g$ —the region occupied only by interconnecting GAGs;  $\Omega_c$ —the region occupied only by the coating GAGs

where  $e$  is the unit charge supplied by the disaccharide unit. The uniform charge density for the coating GAGs is

$$\rho_c = (1 - \lambda) \frac{\rho_{\text{eff}} Ah}{V_c}, \quad (2.26)$$

where  $h$  is the length and  $Ah$  the volume of the unit cell, respectively. The bridging GAGs repeat along the axis of collagen fibrils with period  $h$ , which may be determined using the conservation of total charge

$$\rho_{\text{eff}} Ah \lambda = \frac{\sum_{i=1}^{N_{\text{gag}}} l_g^i \alpha e}{b}, \quad (2.27)$$

where  $\lambda$  is the charge fraction for the bridging GAGs and  $\sum_{i=1}^{N_{\text{gag}}} l_g^i$  is the total length of the GAG rods over the unit cell. As an example, we employ a next-nearest neighbor topology for the interconnecting GAGs proposed by Muller et al. (2004). The 3-D unit cell model has uniform charge density  $\rho_c$  in the coating domain and  $\rho_g$  in the bridging GAG cylinders (Fig. 2.5).

The Poisson-Boltzmann equation is solved for the electrostatic potential  $\varphi$  over the cell subdomains with boundary conditions as described by Eqs. (2.21) and (2.22) and with fixed charge density  $\rho_f$  prescribed as,

$$\rho_f = \begin{cases} \rho_c & \text{on } \Omega_c, \\ \rho_g & \text{on } \Omega_g, \\ \rho_c + \rho_g & \text{on } \Omega_c \cap \Omega_g, \end{cases} \quad (2.28)$$

and  $\rho_f = 0$  elsewhere. Charge conservation is applied to the bridging and coatings GAGs domains independently. As the unit cell is deformed, the charge density  $\rho_g$  changes due to the cylinder length change. The coating charge density  $\rho_c$  will not change, as discussed above. For simplicity, the GAG radius  $r_g$  is invariant during cell deformation.

**Fig. 2.6** Swelling pressure vs. corneal thickness around the physiological condition ( $t = 0.5$  mm) by the molecular-level unit cell model. The average charge density  $\rho_{\text{eff}}/F = 48$  mM and the radius of the GAGs rod varies from 3 to 5 nm, the ratio  $\alpha = 4.0$  and charge fraction  $\lambda = 0.5$

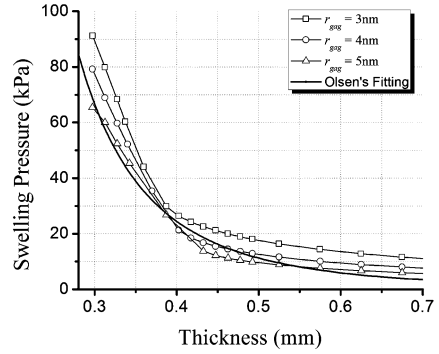


Figure 2.6 shows the computed swelling pressure versus the tissue thickness. The cell effective charge density is taken to be  $\rho_{\text{eff}}/F = 48$  mM. The interfibrillar spacing  $l_c = 53$  nm, radius of the collagen fibril  $r_c = 12.5$  nm, and the coating radius  $r_c = 18$  nm have the same values used in the previous models. The molecular length ratio is taken to be  $\alpha = 4.0$ , and the charge partition fraction  $\lambda = 0.5$ . We have studied the model under GAGs radii varying from 3 to 5 nm. The sensitivity of the results with respect to  $r_g$  is presented in Fig. 2.6. An increase in the effective GAG radius leads to a decrease in the computed swelling pressure, as expected, because the charge density  $\rho_g$  in the GAG cylinders drops. From Fig. 2.6, we observe that  $r_g = 3 \sim 4$  nm gives a result that matches the experimental curve well.

## 2.5 Discussion

In this work we have compared predictions for equilibrium swelling pressure of the human stroma using three models. Each model provides a representation of the electrostatic forces arising from the charges associated with the linear GAG chains of the tissue PGs and with the mobile ions in the polyelectrolyte phase. The first to be considered was a continuum model based on Donnan equilibrium which requires the electrostatic potential to be spatially invariant. This allows no representation of molecular-level or microstructural-level information. This model was based on a uniform fixed charge density that has been reported from independent experimental measurement. The model equates the Donnan osmotic pressure difference between the polyelectrolyte phase and bath with the swelling pressure. The prediction for equilibrium swelling pressure at physiological hydration is reasonable but the approach severely underestimates swelling pressure at lower hydration levels.

The second model is also a continuum model. It is a unit cell approach and based on a thermodynamic derivation for the swelling pressure in which the swelling pressure emerges as the derivative of the electrostatic free energy with respect to the swelling volume. In this model, the electrostatic potential is found from the Poisson-Boltzmann equation. This model contains no molecular-level information but does describe the microstructure of the tissue. In particular, it accounts for the polyelectrolyte phase being excluded from the volume occupied by collagen fibrils. As the

hydration reduces, the volume containing the fixed charges decreases due to a geometrical effect. This model provides an accurate swelling pressure prediction over all ranges of hydration. The model is further improved by partitioning the charge into two GAG-based groups: one associated with a charge-dense coating of the collagen fibrils, in accordance with experimental evidence, and one dispersed over the interfibrillar volume and associated with GAGs which bridge fibrils, possibly by duplexing. This refinement gives a surprisingly accurate prediction for swelling pressure at  $\lambda = 0.6$ , when 40 % of the charge is in the coating region. This result implies that around physiological hydration ( $t = 0.5$  mm), the swelling pressure primarily results from the bridging GAGs in the interfibrillar region. As the tissue is compressed toward  $t \sim 0.25$  nm, the coatings start to play a role by mutually interacting and producing a local increase in charge density and a concomitant increase in swelling pressure.

The third model employs a molecular-level unit cell in which volumetric domains within the unit cell are associated with the macromolecular GAGs. The model is a hybrid approach in that it represents the fibril coating as a charge-dense region around the fibrils using a continuum description. The approach accounts for the spatially varying electrostatic potential between the explicit GAG domains and the mobile ions, again using the Poisson-Boltzmann equation. The results of this model applied to the case of next-nearest neighbor GAG connectivity, as proposed by Muller et al. (2004), are also quite accurate. This approach does introduce additional variables that are not readily estimated, including the GAG length ratio  $\alpha$ , which describes the waviness of the GAG chains, and the radius of the effective GAG cylinder  $r_g$ . However, the length ratio  $\alpha$  for the bridging GAGs is also a relevant parameter for estimating the entropic elasticity of the polymer chain using a theory such as the wormlike chain model.

In the present study, we have addressed the swelling problem in terms of the electrostatic component of the free energy alone. However, the chemomechanical free energy, which includes the entropic elasticity of the GAGs and the molecular mixing energy, will certainly have some influence on the swelling pressure (Hart and Farrell, 1971; Jin and Grodzinsky, 2001). Indeed, the GAG entropic elasticity will produce expansion-resisting forces that will contribute a ‘negative’ swelling pressure component (Hart and Farrell, 1971). These non-electrostatic components will be the subject of a future study.

**Acknowledgements** This research was supported by the Stanford University Bio-X Interdisciplinary Initiatives Program (PMP), which is gratefully acknowledged. XC also received support from a Stanford Graduate Fellowship.

## References

- Buschmann MD, Grodzinsky AJ (1995) A molecular model of proteoglycan-associated electrostatic forces in cartilage mechanics. *J Biomech Eng* 2:179–192
- Che J, Dzubiella J, Li B, McCammom JA (2008) Electrostatic free energy and its variations in implicit solvent models. *J Phys Chem B* 112:3058–3069

- Elliott GF, Hodson SA (1998) Cornea, and the swelling of polyelectrolyte gels of biological interest. *Rep Math Phys* 61:1325–1365
- Fatt I (1968) Dynamics of water transport in the corneal stroma. *Exp Eye Res* 7:402–412
- Fogolari F, Briggs JM (1997) On the variational approach to Poisson-Boltzmann free energies. *Chem Phys Lett* 281:135–139
- Fratzl P, Daxer A (1993) Structural transformation of collagen fibrils in corneal stroma during drying. *Biophys J* 64:1210–1214
- Hart RW, Farrell RA (1971) Structural theory of the swelling pressure of corneal stroma in saline. *Bull Math Biophys* 33:165–186
- Hedbys BO, Dohlman C (1963) A new method for the determination of the swelling pressure of the corneal stroma in *in vitro*. *Exp Eye Res* 2:122–129
- Hedbys BO, Mishima S (1966) The thickness-hydration relationship of the cornea. *Exp Eye Res* 5:221–228
- Hodson S (1971) Why the cornea swells. *J Theor Biol* 33:419–427
- Jin M, Grodzinsky AJ (2001) Effect of electrostatic interactions between glycosaminoglycans on the shear stiffness of cartilage: a molecular model and experiments. *Macromolecules* 34:8330–8339
- Katchalsky A, Michaeli I (1955) Polyelectrolyte gels in salt solutions. *J Polym Sci* 15:69–86
- Lewis PN, Pinali C, Young RD, Meek KM, Quantock AJ, Knupp C (2010) Structural interactions between collagen and proteoglycans are elucidated by three-dimensional electron tomography of bovine cornea. *Structure* 18:239–245
- Meek KM, Leonard DW (1993) Ultrastructure of the corneal stroma: a comparative study. *Biophys J* 64:273–280
- Muller LJ, Pels E, Schurmans L, Vrensen G (2004) A new three-dimensional model of the organization of proteoglycans and collagen fibrils in the human corneal stroma. *Exp Eye Res* 78:493–501
- Olsen T, Sperling S (1987) The swelling pressure of the human corneal stroma as determined by a new method. *Exp Eye Res* 44:481–490
- Scott JE (1992) Morphometry of cupromeronic blue-stained proteoglycan molecules in animal corneas, versus that of purified proteoglycans stained *in vitro*, implies that tertiary structures contribute to corneal ultrastructure. *J Anat* 180:155–164
- Twersky V (1975) Transparency of pair-correlated, random distributions of small scatterers, with applications to the cornea. *J Opt Soc Am A* 65:524–530



<http://www.springer.com/978-94-007-5463-8>

Computer Models in Biomechanics

From Nano to Macro

Holzapfel, G.; Kuhl, E. (Eds.)

2013, XII, 416 p., Hardcover

ISBN: 978-94-007-5463-8